Journal of Cellular Biochemistry 97:1241–1258 (2006)

Structural Specificity in a FGF7-Affinity Purified Heparin Octasaccharide Required for Formation of a Complex with FGF7 and FGFR2IIIb

Yongde Luo,[1] Sheng Ye,[2] Mikio Kan,[4] and Wallace L. McKeehan[1,3]*

[1]Center for Cancer Biology and Nutrition, Institute of Biosciences and Technology, The Texas A&M University System Health Science Center, Houston, Texas
[2]Center for Structural Biology, Institute of Biosciences and Technology, The Texas A&M University System Health Science Center, Houston, Texas
[3]Department of Biochemistry and Biophysics, Texas A&M University, Houston, Texas 77030-3303
[4]Zeria Pharmaceutical Co., Ltd., Saitama, Japan

Abstract Variations in sulfation of heparan sulfate (HS) affect interaction with FGF, FGFR, and FGF–HS–FGFR signaling complexes. Whether structurally distinct HS motifs are at play is unclear. Here we used stabilized recombinant FGF7 as a bioaffinity matrix to purify size-defined heparin oligosaccharides. We show that only 0.2%–4% of 6 to 14 unit oligosaccharides, respectively, have high affinity for FGF7 based on resistance to salt above 0.6M NaCl. The high affinity fractions exhibit highest specific activity for interaction with FGFR2IIIb and formation of complexes of FGF7-HS-FGFR2IIIb. The majority fractions with moderate (0.30–0.6M NaCl), low (0.14–0.30M NaCl) or no affinity at 0.14M NaCl for FGF7 supported no complex formation. The high affinity octasaccharide mixture exhibited predominantly 7- and 8-sulfated components (7,8-S-OctaF7) and formed FGF7–HS–FGFR2IIIb complexes with highest specific activity. Deduced disaccharide analysis indicated that 7,8-S-OctaF7 comprised of ΔHexA2SGlcN6S in a 2:1 ratio to a trisulfated and a variable unsulfated or monosulfated disaccharide. The inactive octasaccharides with moderate affinity for FGF7 were much more heterogenous and highly sulfated with major components containing 11 or 12 sulfates comprised of predominantly trisulfated disaccharides. This suggests that a rare undersulfated motif in which sulfate groups are specifically distributed has highest affinity for FGF7. The same motif also exhibits structural requirements for high affinity binding to dimers of FGFR2IIIb prior to binding FGF7 to form FGF7–HS–FGFR2IIIb complexes. In contrast, the majority of more highly sulfated HS motifs likely play FGFR-independent roles in stability and control of access of FGF7 to FGFR2IIIb in the tissue matrix. J. Cell. Biochem. 97: 1241–1258, 2006.

Key words: extracellular matrix; FGF signaling; glycobiology; heparan sulfate; proteoglycans; tyrosine kinases

Abbreviations used: 7,8-S-OctaF7, octasaccharide from FGF7 affinity containing 7 or 8 sulfate groups; DMB, 1,9-dimethylmethylene blue; DSS, disuccinimidyl suberate; FGF, fibroblast growth factor; FGFR, fibroblast growth factor receptor tyrosine kinase; FHR, complex of FGF, heparan sulfate motif and FGFR; GAG, glucosaminoglycan; GlcA, glucuronic acid; GlcN, 2-N-unsubstituted glucosamine; GlcN3S, 3-*O*-sulfated glucosamine; GlcN6S, 6-*O*-sulfated glucosamine; GlcNAc, 2-N-acetylated glucosamine; GlcNS, 2-N-sulfated glucosamine; GST, glutathione-S-transferase; HS, heparan sulfate; ΔHexA2S, 2-*O*-sulfated uronic acid with a C4-C5 unsaturated bond; IdoA, iduronic acid; IPRP-HPLC, ion pairing reverse phase high performance liquid chromatography; LMWH, low molecular weight heparin; MALDI-TOF-MS, matrix assisted laser desorption ionization time-of-flight mass spectrometry; PIMH or H, porcine intestinal mucosa heparin; UA, uronic acid containing isomers of IdoA and GlcA.

Grant sponsor: National Institute of Diabetes and Digestive Diseases; Grant number: DK35310; Grant sponsor: National Cancer Institute; Grant number: CA59971; Grant sponsor: GS PlatZ, Ltd., Tokyo, Japan.

*Correspondence to: Wallace L. McKeehan, Center for Cancer Biology and Nutrition, Institute of Biosciences and Technology, The Texas A&M University System Health Science Center, 2121 W. Holcombe Blvd., Houston, TX 77030-3303. E-mail: wmckeehan@ibt.tamhsc.edu

Received 12 September 2005; Accepted 18 October 2005
DOI 10.1002/jcb.20724

The fibroblast growth factor (FGF) signal transduction system is ubiquitous and plays wide biological roles in embryonic development and adult tissue homeostasis [McKeehan et al., 1998; Ornitz, 2000]. Defects in the family are associated with tissue-specific diseases. The FGF signaling complex is an oligomeric structure comprised of subunits of activating FGF polypeptide, transmembrane receptor tyrosine kinase (FGFR), and motifs within heparan sulfate (HS) [Kan et al., 1999; Pellegrini et al., 2000; Schlessinger et al., 2000]. Twenty-two FGF homologs and 4 FGFR tyrosine kinase genes have been identified in humans and mice [Itoh and Ornitz, 2004]. Combinations of alternative splice events also contribute to functional diversity of FGFR [McKeehan et al., 1998]. Least is known about the diversity and specificity of oligosaccharide motifs within the HS subunit that derives from linear chains of disaccharide repeats of proteoglycans on the cell surface and in the extracellular matrix [Lindahl et al., 1998; Esko and Selleck, 2002]. HS disaccharide repeats consist of 2-hydroxy sulfates on glucuronate (GlcA) and iduronate (IdoA), 2-amino, 3-hydroxy and 6-hydroxy sulfates on glucosamine (GlcN), and acetate on the 2-amino of GlcN [Lindahl et al., 1998; Linhardt, 2003]. Modifications at all positions are incomplete and occur to different extents dependent on the source of HS. Next to the interaction with antithrombin (ATIII) in prevention of clotting and maintenance of blood flow [Kuberan et al., 2003; Petitou et al., 2003], the interaction of HS with FGF and FGFR and its impact on FGF signaling has received the most attention of over 100 reported proteins [Capila and Linhardt, 2002; Powell et al., 2004]. Numerous studies using diverse experimental approaches from biochemical to physiological indicate that variations in extent and type of sulfation within HS impact the independent interaction with different FGFs [Kreuger et al., 2001; Ye et al., 2001], FGFRs [Powell et al., 2002], and the formation of signaling complexes of FGFs and FGFRs [Guimond and Turnbull, 1999; Kan et al., 1999; Ostrovsky et al., 2002; Wu et al., 2003]. It is unclear whether specific distribution of sulfates rather than non-specific variations in total charge density within chains of HS plays a role in context-specificity of control of FGF signaling. To date the former has only been demonstrated for antithrombin-mediated anticoagulation [Hurst et al., 1979; Petitou et al., 2003].

Experimental systems where the interactions of FGF and FGFR are dependent on HS and affinity of HS motifs for FGF and FGFR is high (Kd $<10^{-8}$M) are essential to assess the structural role of HS in assembly of the FGF signaling complex. Since 1993, we have employed a eukaryotic insect cell expression system comprised of membrane-anchored dimers of the FGFR ectodomain and transmembrane domain fused to GST dimers on the intracellular C-terminus. The properties of the FGFR-GST dimers can be maintained for short times anchored to GSH-beads after extraction from membranes [Kan et al., 1996]. In this system, the binding of FGF to dimeric FGFR is dependent on HS and has an affinity for HS of 10 nM or better. Moreover, the FGFR ectodomains selectively interact with a minority fraction of HS or heparin mixtures that is enriched in anticoagulant activity. This is in contrast to soluble ectodomains from both mammalian [Berman et al., 1999; LaRochelle et al., 1999] and insect cells [Loo et al., 2000, 2001], or refolded insoluble bacterial expressed products [Pellegrini et al., 2000; Schlessinger et al., 2000]. On an analytical scale, the experimental system has revealed the functional importance of targeting FGFR to cell membranes in eukaryotic cells, and the presence of the extracellular juxtamembrane and transmembrane domains. This and anchorage to membranes or solid matrices as dimers appears essential for the high affinity interaction of HS with the FGFR ectodomain, and the dependence on HS for FGF binding to FGFR. The HS-dependent system also revealed an essential HS binding sequence in immunoglobulin module II of the FGFR ectodomain [Kan et al., 1993]. It further revealed a FGFR-, FGF-, and cell-type specificity of FGFR–HS complexes for FGF [Kan et al., 1999, 2001]. Despite these advantages as a recombinant analytical system, scalability has limited direct affinity purification of specific FGFR-interactive HS oligosaccharide motifs for structure-function analyses using FGFR as the affinity reagent.

More recently, resolution of the crystal structures and molecular modeling has revealed unique HS-binding domains in FGF7, FGF9 [Plotnikov et al., 2001], and FGF19 [Harmer et al., 2004b] relative to widely studied prototypes FGF1 and FGF2, and other FGFs such as FGF4, FGF8, and FGF10 [Ye et al., 2001]. HS-binding domains in FGF7, FGF9, and FGF19

are characterized by significantly reduced basicity and dispersion of remaining basic residues among intervening uncharged or acidic residues. This predicted a more stringent structural requirement of FGF7 for HS motifs with a specific distribution of sulfate groups along the linear oligosaccharide chain. Consistent with this prediction, we found that in contrast to FGF1, heparin oligosaccharides of 10–14 in length containing a 3-*O*-sulfate were most active in protection of FGF7 against protease [Ye et al., 2001]. Moreover, the recombinant GST-FGF7 precursor [Luo et al., 2004], which was used successfully for resolving the native FGF7 structure, selectively enriched the antithrombin-mediated inhibition of Factor Xa activity (referred to as anticoagulant activity) from crude stocks of heparin with an effectiveness equal to antithrombin [Ye et al., 2001; Luo et al., 2003]. Since this property was in common with heparin and rat liver HS that bound FGFR with highest affinity [McKeehan et al., 1999], we hypothesized that the high affinity oligosaccharides specific for FGF7 may also be those forming HS–FGFR2IIIb complexes into which FGF7 binds to form the FGF7–HS–FGFR2IIIb complex.

To test this idea we exploited the unique heparin-binding domain, high yield, and stability of precursor GST-FGF7 [Luo et al., 2004] to overcome the scalability limits of insect cell FGFR as an affinity matrix. Heparin oligosaccharide fractions with graded affinity for FGF7 based on salt resistance were monitored for ability to support binding of FGF7 to FGFR2IIIb. An octasaccharide with highest affinity for FGF7 was the shortest oligosaccharide capable of forming the FGF7-HS-FGFR2IIIb complex and the longest in which near homogeneity in respect to sulfation could be achieved. Biochemical analysis revealed that the high affinity octasaccharide was an undersulfated mixture of 7- and 8-sulfated components. It is comprised of the uncommon N-unsubstituted disaccharide ΔHexA2SGlcN6S, a trisulfated disaccharide, and a variable unsulfated or monosulfated disaccharide. In contrast, more abundant, heterogenous, and more highly charged octasaccharides with lower affinity were unable to form FGF7–HS–FGFR2IIIb complexes. The results suggest that rare undersulfated octasaccharide motifs in which sulfate groups are specifically distributed, rather than simply highly charged motifs independent of distribution of sulfates, play a role in assembly of the FGF7 signaling complex.

MATERIALS AND METHODS

HS-Dependent Binding of FGF7 to FGFR2IIIb

Pure high quality recombinant FGF7 was prepared and iodinated as described previously [Kan et al., 1991]. The FGFR2IIIb ectodomain including the extracellular juxtamembrane and transmembrane domains fused to GST on the C-terminus was expressed into the membranes of baculoviral-infected Sf9 cells. Specific binding of ^{125}I-FGF to FGFR was distinguished from nonspecific binding by the difference between infected and uninfected cells. The specific binding was confirmed by covalent affinity crosslinking between FGF7 and FGFR2IIIb using the bidirectional amine-reactive crosslinker DSS containing 11.4 Å spacer arms [Wang et al., 1995]. Binding to uninfected and mock infected cells or cells expressing FGFR2IIIb in the absence of HS was generally 10%–15% of the maximal binding on cells expressing FGFR2IIIb in the presence of HS. No radiolabeled complexes of FGF and FGFR could be detected by covalent affinity crosslinking on uninfected cells or infected cells in absence of heparin. Cell free experiments were performed by detergent extraction of membrane bound FGFR2IIIb-GST dimers and immobilization on GSH-beads followed by incubation with HS fractions and extensive washing to eliminate material bound with low affinity prior to addition of ^{125}I-FGF7 [Kan et al., 1999]. The affinity of cell free FGFR2IIIb-GST dimers for HS with Kd $<$10 nM and dependence on HS for FGF7 binding were routinely employed as a measure of quality and utility of the assay system. Except where dose response curves were performed, 0.3 μM of oligosaccharides from different fractions was added to the binding mixtures. Binding activity in the presence of 0.4 μg/ml crude heparin, the minimal amount that promoted maximum binding in a dose response curve, was designated as 100% output of the binding assay, which represented 6,000 cpm of ^{125}I-FGF7. Experiments were repeated at least three times with samples from at least three independent preparations (minimum nine determinations).

Heparin Oligosaccharide Mixtures of Defined Length

About 1.0 g of porcine intestinal mucosal heparin (6,000–30,000 Da, 170 USP units/mg;

Sigma, St. Louis, MO) was dissolved in 10 ml buffer of 100 mM sodium acetate, 25 mM calcium acetate, pH 7.4, and 1 mM DTT, and filtered through 0.22 μm Tuffryn Membranes (Pall Corporation, Ann Arbor, MI). After addition of 40 Sigma units of heparinase 1 (Sigma), the mixture was incubated for about 18 h at 37°C to achieve a 10%–30% partial digest. Progress of the digestion was monitored by the increase in absorbance at 226 nm resulting from the double bond formation between C4 and C5 positions on the non-reducing end after the β-elimination endolytic cleavage. The heparinase 1 was inactivated by exposure of the mixture to 75°C for 5 min.

About 200–300 mg of the digested mixture was applied to a Bio-Gel P-10 (Bio-Rad, Hercules, CA), polyacrylamide-based size-exclusion matrix housed in tandem XK26/100 columns (26 mm × 200 cm; Amersham Pharmacia Biotech, Piscataway, NJ). The packed Bio-Gel P-10 column was calibrated with a synthetic antithrombin-binding pentasaccharide (AT5) (a gift from Dr. Robert Linhardt) and disaccharide standards (Sigma). V_0 and V_t were determined by blue dextran (MW, 2,000 kDa) and acetone (MW, 58 Da), respectively. Oligosaccharides up to a hexadecasaccharide were separated using an FPLC System (Amersham Pharmacia Biotech) in a mobile phase of 0.2M NH_4HCO_3. The central portion of each peak corresponding to an individual type of HS oligosaccharide was collected, heated at 70°C for 1 h, and freeze-dried. The dried powder from each peak was dissolved in water and subjected to the same chromatographic procedure. After collection of the center portion of each single peak, the sample was freeze-dried, dissolved in water, and desalted on a 5 ml Sephadex G-25 column (Amersham Pharmacia Biotech) and again freeze-dried. The amount of oligosaccharide was estimated from concentration curves using the dry weight of porcine intestinal heparin (PIMH) as the standard. Sulfate content was first estimated using 1,9-dimethylmethylene blue (DMB) (Biocolor Ltd., Newtownabbey, Northern Ireland) staining. Uronic acid content was then quantified using a modified H_2SO_4-borate-carbazol assay. Concentration of crude heparin mixtures was expressed by weight and that of oligosaccharides was expressed in molarity.

Purity of each oligosaccharide fraction in respect to size was assessed by analysis on 16%–36% gradient polyacrylamide gel electrophoresis (PAGE) with an upper chamber buffer of 0.2M Tris and 1.24M glycine and a lower chamber buffer of 0.1M Tris-HCl (pH 8.3), 1M boric acid, and 0.01M EDTA. Samples were applied in a solution of 50% sucrose, 0.04% bromophenol blue, and 0.4% phenol red and run with constant cooling at 200–400 V for 4 h. Oligosaccharides were visualized by Alcian Blue staining followed by destaining background with 5% acetic acid. Homogeneity in respect to size was also monitored by Matrix-assisted Laser Desorption Ionization Time-of-Flight Mass Spectrometry (MALDI-TOF-MS). Twice-chromatographed oligosaccharide fractions exhibiting heterogeneity were subjected to further purification on the Bio-Gel P-10 column until homogeneity was apparent.

Inhibition of Factor Xa Activity

Antithrombin-mediated inhibition of Factor Xa activity was performed as described [Luo et al., 2003] and referred to as anticoagulant activity throughout the manuscript. The Factor Xa activity in the presence of antithrombin, but absence of heparin oligosaccharides was defined as 100% activity that represented about 540 A405 milliunits. Experiments were generally performed at least three times with each of at least three independent oligosaccharide preparations.

FGF7-Affinity Chromatography

Methods for high yield production and recovery of stabilized recombinant rat FGF7 fused at the N-terminus with GST in bacteria has been described in detail [Luo et al., 2003, 2004]. An FGF7 affinity matrix was prepared by bioimmobilization of GST-FGF7 on GSH-Sepharose [Luo et al., 2003]. Prior to use, the FGF7 affinity column was washed with linear gradients of 0.14 to 1.3M, then 1.3 to 0.14M of NaCl in buffer A of 10 mM Tris-HCl (pH 7.4), 0.1 mM DTT and 0.02% NaN_3 at 1 ml/min, and equilibrated in buffer A containing 0.14M NaCl.

One to five milligram of size-defined heparin octasaccharide, decasaccharide, dodecasaccharide or tetradecasaccharide mixtures were dissolved in buffer A containing 0.14M NaCl and applied to the FGF7 affinity columns at 0.3 ml/min. The oligosaccharide load was maintained at an estimated 1:1 molar ratio to immobilized FGF7. After collection of the unretained flow-through at 0.14M NaCl, bound

oligosaccharides were then eluted stepwise at 0.3, 0.6, 1.0, and 1.3M NaCl [Luo et al., 2003]. The eluate between 0.14 and 0.30M, 0.30 and 0.60M, and 0.60 and 1.0M NaCl was arbitrarily defined as the low, moderate, and high affinity fractions, respectively. Elution at each step was continued until absorbance at 226 nm returned to baseline. Fractions were freeze-dried and desalted on Sephadex G-25 with water as the mobile phase. Each dried fraction was reconstituted and then subjected to a second round of FGF7 affinity purification on a fresh column. Oligosaccharides were detected during elution by UV absorbance at 226 nm. The quality and specificity of GST-FGF7 affinity columns was judged by yield of material eluting between 0.60 to 1.0M salt. Post-fractionation quality controls of the FGF7 used in chromatography was performed by analysis of activity of the FGF7 recovered from immobilized GST-FGF7 by on-column trypsin treatment in the presence of protective heparin. About 70% of immobilized FGF7 was recovered that exhibited heparin-dependent FGFR2IIIb binding in the pM range and intact mitogenic activity for mouse keratinocytes from high yield columns (about 0.7% for the high affinity octasaccharide).

Strong Anion-Exchange (SAX) HPLC

Each fraction of octasaccharide at 100 μg except the 1.0M fraction which was at 10 μg from FGF7 affinity chromatography was applied to a Propac PA1 column (4 × 250 mm) (Dionex, Sunnyvale, CA) and eluted with a linear gradient of NaCl from 0 (pump A1) to 2.0M (pump B1) in H_2O-HCl (18.2 megohms/cm at 25°C, pH 3–3.5) over a period of 160 min at 1 ml/min on the AKTApurifier monitored at 226 nm. Oligosaccharide fractions corresponding to individual peaks were pooled, desalted and freeze-dried. The chromatographic data for different octasaccharide fractions from one of three runs for each of three preparations were aligned and stacked into one plot by the automatic Unicorn 3.21 HPLC evaluation program (Amersham Pharmacia Biotech).

Mass Spectrometry

Molecular mass analysis was determined by MALDI-TOF-MS (Bruker Daltonics, Inc., Billerica, MA). About 10 ng of purified octasaccharide in 2 μl water was mixed with 1 μl containing 50 ng of the basic carrier peptide $(Arg\text{-}Gly)_{19}\text{-}Arg$ [calculated mass of the deprotonated $(M+H)^+$ ion = 4,225.6] (Sigma-Genosys Ltd., Houston, TX) that was about a 1:3 molar ratio in 0.1% TFA and 4 μl matrix solution comprised of 15 mg/ml caffeic acid in 40% aqueous acetonitrile. The carrier peptide protects the sugar chain and side groups, enhances the signal output and serves as an internal standard [Juhasz and Biemann, 1995]. The mass of oligosaccharides was calculated by difference between the complex and free peptide. The number of sulfate (N_{SO3}) and acetyl (N_{OAc}) groups was calculated based on a formula of $[m/z = 4{,}225.61 + 337.29N + 80.06N_{SO3} + 42.04N_{OAc}]$, given $z = 1$, and N, N_{SO3}, and N_{OAc} are all positive integers. A 2 μl mixture was deposited on polished stainless steel chip, air-dried, and analyzed by AutoFLEX MALDI-TOF-MS. The instrument was set to linear and positive deflection mode with 120 ns delayed extraction and an average 120 shots. The mass gate was set to 2,000 Da. The mass spectrum was also calibrated by external peptide standards angiotension II and somatatostatin with reference masses of 1,046.54 and 3,148.47 Da, respectively. Data were processed and evaluated by XMASS (Bruker Daltonics, Inc.), which generated a plot of m/z (X-axis) versus relative intensity (RI). Since MALDI usually produces a single deprotonated ion, the m/z is equal to the recorded mass value. RI is defined as relative value of the highest counts detected in the same run that was assigned a value of 1. About 10 mass chromatograms were generated from each of at least three independent preparations of oligosaccharides fractionated on independent GST-FGF7 affinity columns.

Disaccharide Analysis

Oligosaccharides were completely digested to disaccharides using heparinase 1, 2, and 3 in a buffer of 10 mM ethylenediamine, 1 mM calcium acetate, and 1 mM DTT adjusted to pH 7.0 with glacial acetic acid. Solvent was removed by evaporation. After desalting on Sephadex G-25 columns in water and concentration by centrifugal evaporation, the disaccharide composition was analyzed by strong anion exchange (SAX) chromatography as described for oligosaccharides. The gradient program for the mobile phase was to 25% B1 over 60 min, then to 50% B1 over 10 min followed by increase to 100% B1 over 10 min at a flow rate of 1 ml/min. The column was then washed with a gradient from 100% B1 to 0.2% B1 over 5 min and re-equilibrated with 0.2% B1

for 10 min. The identity of each peak was determined by comparing retention volume to those of 12 types of heparin and HS disaccharide standards (Sigma).

Disaccharide composition was further analyzed by ion-pair reverse phase HPLC (IPRP-HPLC) on a Supelcosil LC-18 column (4.6 × 250 mm) (Supelco, Bellefonte, PA) connected to a Spheri-5 RP-18 pre-column (4.6 × 30 mm) housed in 3 cm MPLC holder (Brownlee Labs). A gradient elution was performed using a binary mobile phase system comprised of 20% (v/v) aqueous acetonitrile (pump A2) and 75% (v/v) aqueous acetonitrile (pump B2). Tetrabutylammonium hydroxide from a 40% solution was added to 0.01M in both A2 and B2 and adjusted to pH 6.7 by phosphoric acid. The multi-step gradient scheme for the mobile phase was established using the best separation of heparin disaccharide standards determined in pilot runs. The program employed was isocratic elution with 100% A2 for 7 min, gradient elution to 27% B2 over 40 min, gradient to 37% B2 over 3 min, gradient to 55% B2 over 30 min, followed by a gradient to 100% B2 over 10 min at a flow rate of 1.2 ml/min. The column was returned to 100% A2 over 5 min, and then continued for 10 min. The column eluate was monitored by absorbance at 226 nm. Disaccharide analysis was performed three or more times on each of at least three independent oligosaccharide preparations from independent GST-FGF7 columns.

Disaccharide mixtures were analyzed by MALDI-TOF-MS as described above for oligosaccharides.

RESULTS

High Affinity Heparin for FGF7 Has Highest Activity for Interaction With FGFR2IIIb and Assembly of FGF7–Heparin–FGFR2IIIb Complexes

Heparin preparations were subjected to affinity chromatography by graded salt elution from GST-FGF7 immobilized to GSH beads [Luo et al., 2003]. The fraction with highest affinity based on salt resistance exhibited the highest activity in support of ^{125}I-FGF7 binding to insect cells expressing membrane-anchored FGFR2IIIb-GST dimers (Fig. 1). About 130 ng/ml of the high affinity fraction that represented about 20% of crude low molecular weight heparin (LMWH) supported half-maximal binding of ^{125}I-FGF7

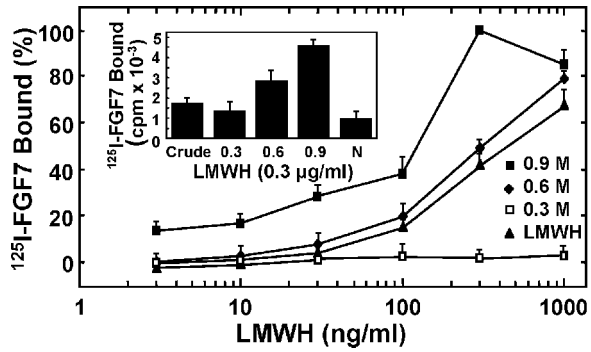

Fig. 1. Increased FGF7–HS–FGR2IIIb complex formation with increased affinity for FGF7. Low molecular weight heparin (LMWH) fractions that eluted stepwise from FGF7 at the indicated concentrations of NaCl were compared to unfractionated LMWH [Luo et al., 2003] for support of ^{125}I-FGF7 binding to recombinant FGFR2IIIb-GST (Materials and Methods). The bound FGF7 was expressed as percent of the peak binding value (100%) that could be achieved with the 0.9M NaCl eluate. *Inset*: Formation of FGF7-binding complexes with cell free immobilized FGFR2IIIb-GST dimers. The amount of ^{125}I-FGF7 bound to blank GSH-beads was subtracted from the total binding to beads bearing immobilized FGFR2IIIb-GST. N, no LMWH added. Data here and in Figures 3–5, 7A, and 8 are the mean ± SD from three experiments performed with three independent oligosaccharide and GST-FGF7 preparations.

compared to 470 ng/ml of crude LMWH. The fraction with moderate affinity for FGF7 (about 40% of the crude LWMH) exhibited activity close to the crude LMWH (310 ng/ml). Activity of the low affinity fraction was negligible. The high affinity fraction for FGF7 was also enriched in ability to bind with high affinity to cell-free dimers of FGFR2IIIb-GST in absence of FGF7. The FGFR2IIIb–LWMH complexes then bound FGF7 (Fig. 1, inset). Results were similar when enoxaparin that is reduced in size from crude heparin by alkaline treatment instead of heparinase was used as source material [Luo et al., 2003].

Activity of Oligosaccharides of Defined Length

Oligosaccharides of defined length were generated from PIMH by controlled heparinase treatment and separated by gel filtration chromatography (Fig. 2). Both FGFR and FGF7 exhibit highest affinity for heparin and HS enriched in anticoagulant activity [McKeehan et al., 1999; Luo et al., 2003]. Therefore, anticoagulant activity was routinely assessed as a monitor of oligosaccharide quality and retention of rare motifs capable of high affinity binding to both FGF7 and FGFR2IIIb. A screen of chemical and enzymatic oligosaccharide production methods revealed that controlled

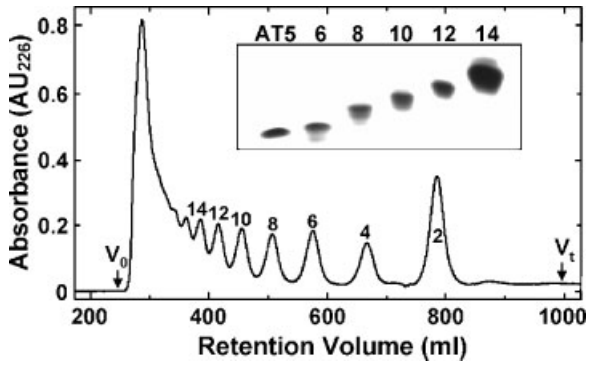

Fig. 2. Generation and purification of oligosaccharide mixtures of defined length. PIMH was subjected to controlled heparinase 1 fragmentation and the resultant oligosaccharides were separated by gel filtration (Materials and Methods). Purity of oligosaccharides in respect to length was monitored by gradient PAGE (inset) and by mass spectrometry. The indicated data is representative of about 6 runs from each of more than 10 independent preparations.

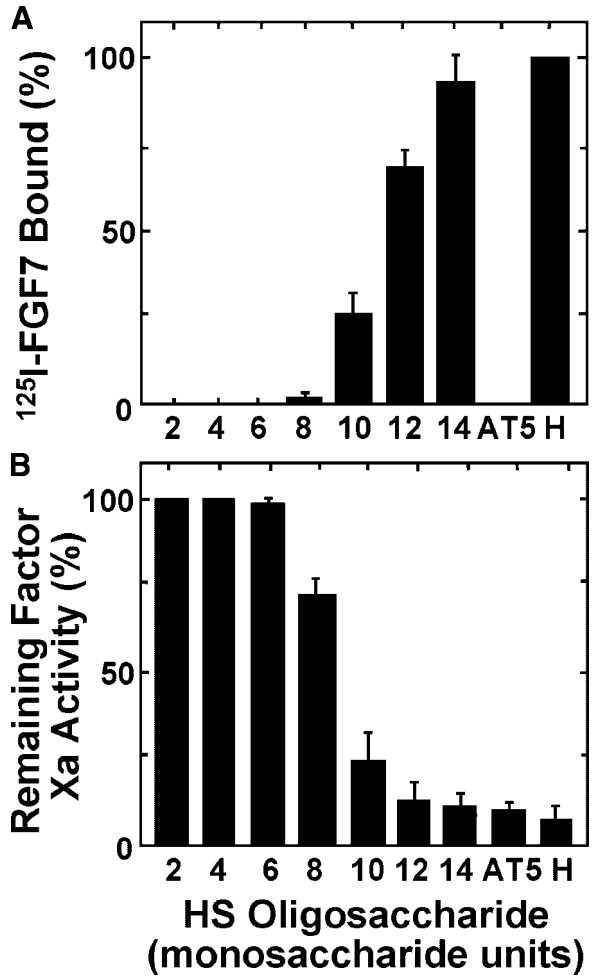

Fig. 3. Ability to support binding of FGF7 to FGFR2IIIb and anticoagulant activity of oligosaccharide mixtures. **A**: FGF7 binding to FGFR2IIIb. Oligosaccharides of the indicated length at 0.3 μM were tested for support of binding of FGF7 to cell surface FGFR2IIIb-GST. Amount of bound radiolabeled FGF7 was expressed as a percentage of that bound in the presence of 0.4 μg/ml crude PIMH (H) (100% values). **B**: Anticoagulant activity. Antithrombin-mediated inhibition of Factor Xa activity of oligosaccharides at 0.3 μM was determined spectrophotometrically (Materials and Methods). Activity is expressed as percent Factor Xa activity in antithrombin and Factor Xa mixtures in absence of heparin. AT5, synthetic AT-binding pentasaccharide at 0.3 μM.

treatment of PIMH with heparinase 1 was the best compromise between total yield of disaccharides to tetradecasaccharides, preservation of anticoagulant activity [McKeehan et al., 1999; Luo et al., 2003], and ability to support FGF7 binding to FGFR2IIIb. Cleavage rate of PIMH was limited to 10%–30% due to the indiscriminate cleavage of the anticoagulant motif and apparently motifs involved in FGF7 signaling by heparinase [Shriver et al., 2000].

We then compared the ability of each oligosaccharide mixture of defined size to support FGF7 binding to FGFR2IIIb. At 0.3 μM, the disaccharide, tetrasaccharide, and hexasaccharide mixtures failed to support detectable FGF7 binding (Fig. 3A). Octa-, deca-, dodeca-, and tetradecasaccharides exhibited 2%, 24%, 70%, and 90% of the activity of 0.4 μg per ml crude PIMH used as a 100% standard. The PIMH standard at 0.4 μg per ml was the lowest concentration required for maximum activity. The synthetic anticoagulant pentasaccharide AT5 failed to support FGF7 binding.

A parallel analysis of anticoagulant activity indicated that activity of the disaccharide, tetrasaccharide, and hexasaccharide mixtures was undetectable at 0.3 μM. The octasaccharide and decasaccharide reduced Factor Xa activity to 25% and 70%, respectively, of 0.3 μM of the synthetic anticoagulant pentasaccharide AT5 that reduced Factor Xa activity to a minimum (100% reduction) (Fig. 3B). Activity of the dodecasaccharide and tetradecasaccharide mixtures was near 90% of the control. This indicates that an octasaccharide is the minimum length that supports assembly of the FGF7–HS–FGFR2IIIb complex. The unfractionated octasaccharide mixture is also the threshold in terms of length for exhibiting significant anticoagulant activity under these assay conditions. The two activities increase in parallel proportional to increasing length of oligosaccharide.

Activity of FGF7-Affinity Purified Size-Defined Oligosaccharides

The oligosaccharides of defined length were then subjected to fractionation on FGF7 affinity columns according to resistance to graded increases in salt concentration (Table I). Retention of disaccharides or tetrasaccharides on FGF7 above 0.6M salt was below the limits of detection. The yield of high affinity oligosaccharide increased progressively with the hexasaccharide (0.2%) through the tetradecasaccharide (4%). Notably the largest increase in yield of oligosaccharides with moderate to high affinity for FGF7 occurs with the increase from 6 to 8 monosaccharide units. The results show that heparin oligosaccharides with high affinity for FGF7 in mixtures ranging in size from disaccharide to tetradecasaccharide are rare with a threshold of detection at the hexasaccharide.

Since the high affinity fraction for FGF7 from crude heparins is enriched in anticoagulant [Luo et al., 2003], we first compared the anticoagulant activity of the oligosaccharide fractions from the FGF7 bioaffinity columns. Similar to the unfractionated hexasaccharide mixture, no activity was detected in the high affinity hexasaccharide (data not shown). At 0.1 μM, the high affinity octasaccharide reduced Factor Xa activity to 60% of that of synthetic anticoagulant pentasaccharide AT5 at 0.1 μM (100% reduction) (Fig. 4). The high affinity decasaccharide and longer oligosaccharides exhibited maximal anticoagulant activity. This was in contrast to the crude octa-, deca-, dodeca-, and tetradecasaccharides that elicited at 0.1 μM, 10%, 37%, 66%, and 75% of maximum anticoagulant activity, respectively. Unretained oligosaccharide fractions at physiological 0.14M salt and the low affinity fractions were devoid of activity independent of size (Fig. 4). Activity of the fractions with moderate affinity increased with size of the oligosaccharide. However, activity of moderate affinity fractions was still less than the average 35% and 85% inhibition, respectively, exhibited by the high affinity and crude oligosaccharide of the same size. These results show that similar to crude heparins [Luo et al., 2003], heparin oligosaccharides of 8 or more units with high affinity for FGF7 are enriched in anticoagulant activity.

The oligosaccharide fractions with graded affinity for FGF7 were then screened for support of assembly of FGF7-heparin oligosaccharide–FGFR2IIIb complexes. Independent of length, unretained oliogosaccharides at physiological salt failed to support binding to FGFR2IIIb (Fig. 5). At 0.3 μM no activity of the high affinity hexasaccharide could be detected (data not shown). Although activity of 0.3 μM of crude octasaccharide was nearly undetectable (Fig. 3), the same amount of high affinity octasaccharide exhibited about 60% of the activity of the PIMH standard (Fig. 5). Activity of the octasaccharide with moderate affinity was near detection limits. Activity of the same amount of high affinity decasaccharide and dodecasaccharide increased to 70% and 120% of the PIMH standard, respectively. The increase in activity of the moderate affinity fractions of the same length was less than 20% of the PIMH standard.

Covalent affinity crosslinking confirmed that only the high affinity oligosaccharides supported the authentic high affinity interaction

TABLE I. Affinity of Oligosaccharides of Defined Length for FGF7[a]

HS oligosaccharide (monosaccharide units)	Percent of applied oligosaccharide			
	NaCl (M)			
	0.14	0.3	0.6	1.0
2	94	5.8	0.2	0
4	56.3	35.6	8.1	0
6	32.4	60.1	7.2	0.2
8	29.4	30.4	39.1	0.7
10	27.2	25.4	45.2	1.2
12	22.8	34.6	38.4	2.5
14	27.8	25.6	40.6	3.7

[a]Oligosaccharides eluting at 0.14, 0.3, 0.6, and 1.0M NaCl were designated as the unretained, low, moderate, and high affinity fractions, respectively.

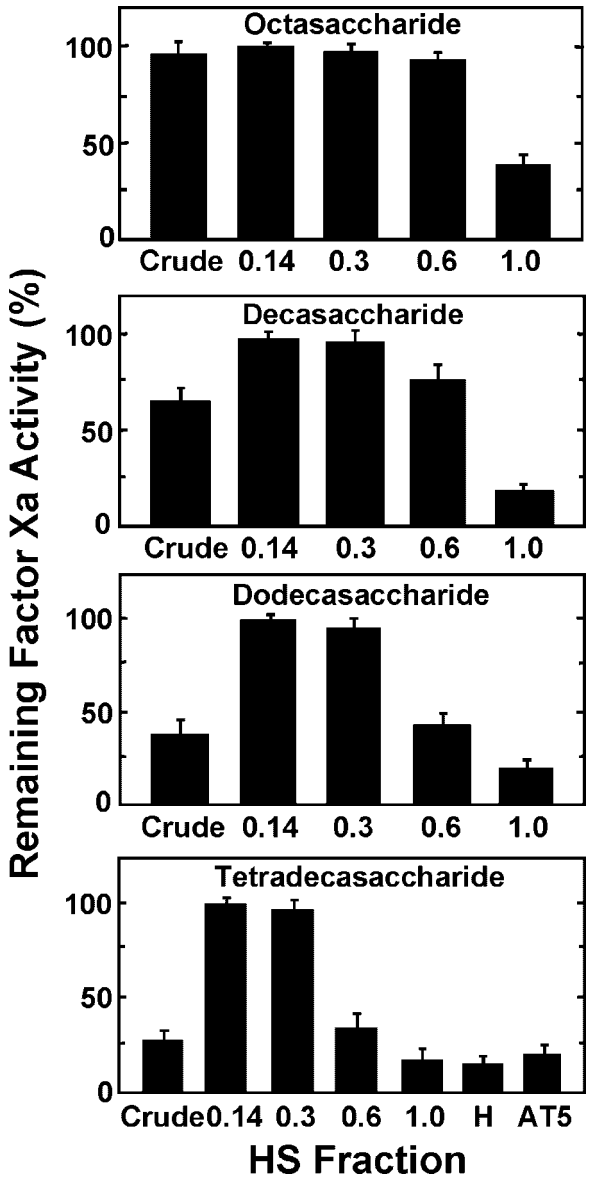

Fig. 4. Anticoagulant activity of FGF7-affinity purified oligosaccharides. The indicated oligosaccharide fractions at 0.1 μM were assayed for anticoagulant activity as in Figure 3B. H, PIMH at 0.13 μg/ml; AT5, synthetic AT-binding pentasaccharide at 0.1 μM.

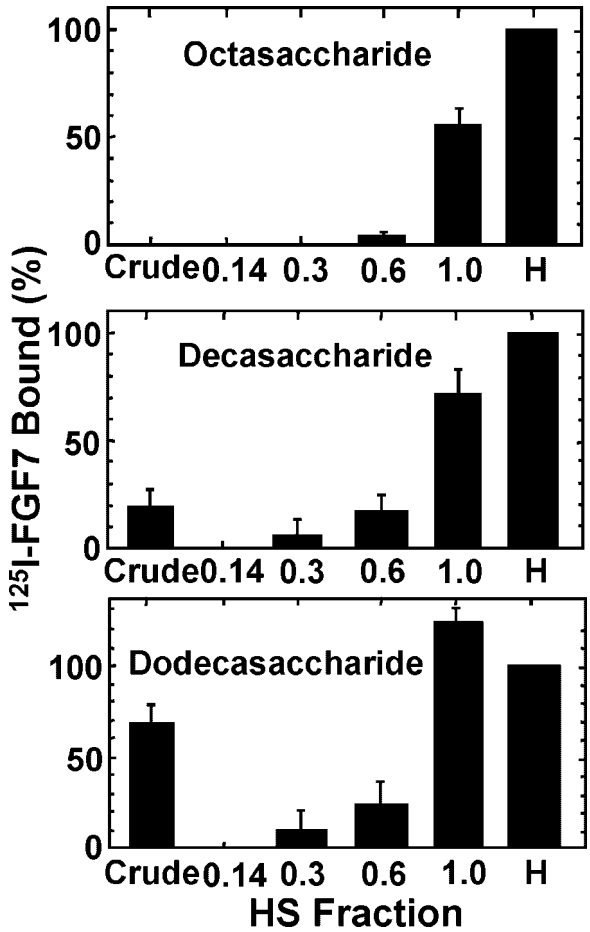

Fig. 5. Activity of oligosaccharide fractions for support of FGF7 binding to FGFR2IIIb. Activity of the indicated fractions of the octasaccharide, decasaccharide, and dodecasaccharide mixtures from FGF7 affinity columns was assessed at 0.3 μM as described in Figure 3A.

of radiolabeled FGF7 with FGFR2IIIb (Fig. 6). As shown for binding to cell surface FGFR2IIIb, only the high affinity fraction of the octasaccharide formed dimeric FGFR2IIIb–octasaccharide complexes that subsequently bound radiolabeled FGF7 (Fig. 7A). Covalent affinity crosslinking also confirmed the authenticity of the high affinity binding of FGF7 to the FGFR2IIIb–octasaccharide complexes (Fig. 7B).

Efficacy of the FGF7-affinity purification procedure for enrichment of activity was evaluated by comparison of the quantitative requirement of purified octasaccharide to the crude octasaccharide for support of FGF7 binding to FGFR2IIIb (Fig. 8). Stimulation of binding could be detected at about 5 nM for the high affinity octasaccharide with a half of maximum and maximum activity at 60 nM and 0.3 μM, respectively. Only about 10% of the maximal activity supported by the high affinity octasaccharide could be achieved with the crude mixture at 3 μM before inhibitory elements dominated. Although this precluded estimation of a quantitative purification factor, the results indicate that the high affinity octasaccharide is many times more active than the crude octasaccharide and fractions with lower affinity for FGF7.

Taken together the results indicate that an oligosaccharide as short as eight monosaccharides supports formation of authentic FGF7–

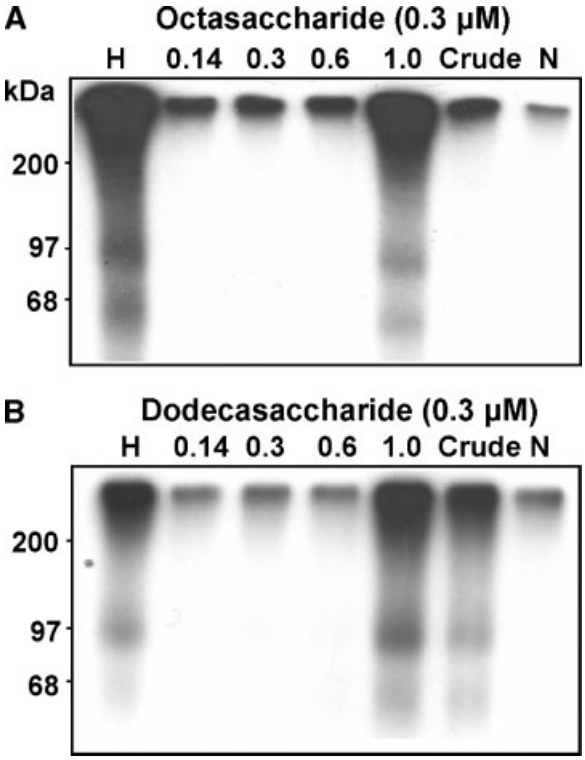

Fig. 6. Only high affinity oligosaccharides for FGF7 support authentic complexes of FGF7 and FGFR2IIIb. **A**: High affinity octasaccharide for FGF7. **B**: High affinity dodecasaccharide for FGF7. Covalent affinity crosslinking of ^{125}I-FGF7 to FGFR2IIIb on the surface of baculoviral-infected insect cells was performed with DSS with concentration of ^{125}I-FGF7 increased from 2 ng/ml to 12 ng/ml. N, no oligosaccharide added. Data are representative of at least three experiments for three independent oligosaccharide and GST-FGF7 preparations.

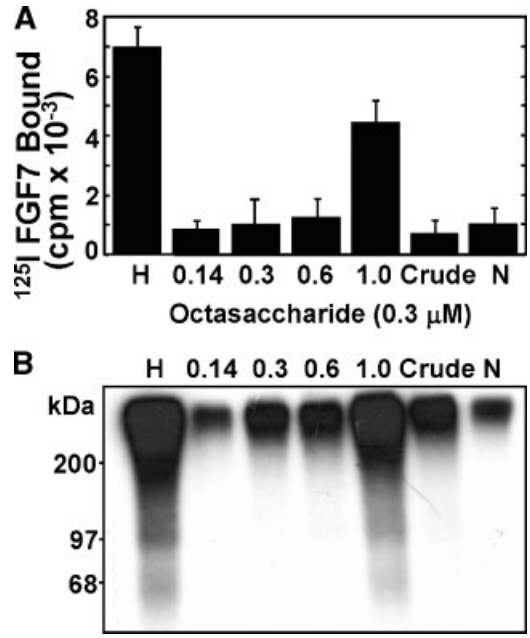

Fig. 7. Only high affinity oligosaccharides for FGF7 bind to FGFR2IIIb for form binary complexes capable of binding FGF7. **A**: Total ^{125}I-FGF7 binding to GSH-beads bearing FGFR2IIIb-GST. Transmembrane FGFR2IIIb-GST was extracted and immobilized on GSH-beads followed by pre-incubation with the indicated octasaccharide fractions at 0.3 μM, removal of unbound oligosaccharide, and introduction of ^{125}I-FGF7 without further addition of oligosaccharides. **B**: Covalent affinity crosslinking of FGF7 with binary complexes of purified octasaccharide and FGFR2IIIb.

HS–FGFR2IIIb complexes. Only a small minority of total heparin octasaccharides contains a motif capable of the high affinity, high salt resistant interaction with FGF7. This rare fraction was also capable of forming stable complexes with dimeric FGFR2IIIb that then bind FGF7. The great majority of octasaccharides with lower affinity for FGF7 do not participate in FGF7–HS–FGFR2IIIb complexes. The results illustrate the high specificity and utility of FGF7 as an affinity reagent to extract rare motifs that participate in formation of the FGF7–HS–FGFR2IIIb signaling complex.

Composition Analysis of FGF7-Affinity Purified Octasaccharides

To determine the nature of the active octasaccharide fraction with high affinity for FGF7 in respect to charge density and sulfation, we subjected the material to analysis by SAX chromatography, MALDI-TOF-MS, and disaccharide composition. SAX analysis indicated that the crude heparin octasaccharide exhibited a distribution of components eluting from about 0.40–1.8M NaCl (Fig. 9). The unretained octasaccharide fraction exhibited components eluting from 0.45 to 1.4M NaCl. The low affinity octasaccharide eluted from 1.2 to 1.8M NaCl with the majority from 1.35 to 1.56M NaCl. The moderate affinity octasaccharide exhibited multiple peaks eluting between 1.65 and 1.8M NaCl with most of the material compressed at the saturation limit of the SAX column (1.8M NaCl) (Fig. 9, top trace). The high affinity octasaccharide exhibited a single signal that was also at the 1.8M NaCl saturation limit. These results indicated both moderate and high affinity octasaccharides for FGF7 cannot be distinguished by SAX chromatography and SAX was of limited utility in assessing differences in charge density, heterogeneity, and further purification.

Therefore the two fractions were subjected to MALDI-TOF mass spectrometric analysis

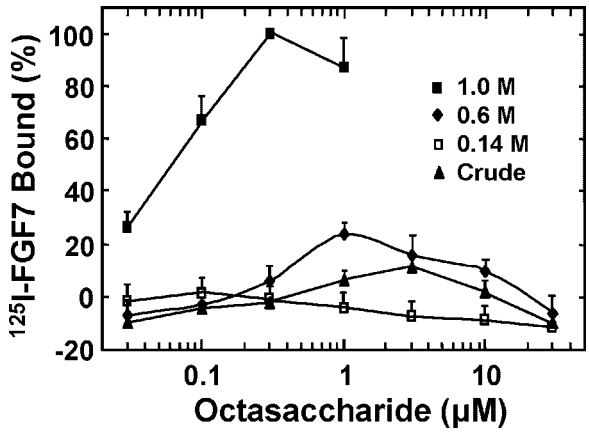

Fig. 8. Specific activity of the FGF7-affinity purified octasaccharide. Activities for support of FGF7 binding to FGFR2IIIb of the octasaccharide fractions at increasing concentration were compared to each other and to crude octasaccharide. The amount of radiolabeled FGF7 bound to cell surface FGFR2IIIb was expressed as a percent of the peak binding supported by the high affinity fraction. Crude, unfractionated octasaccharide mixture.

(Fig. 10). Surprisingly, the active octasaccharide with high affinity for FGF7 exhibited only two predominant signals at experimental m/z of 1,908.47 and 1,987.9 corresponding to octasaccharides with seven and eight sulfates, respectively (Fig. 10, top panel). The signal indicating a 7-sulfated (S)-octasaccharide was notably the strongest. A minor peak coincident in mass with an octasaccharide bearing six sulfates was observed in 85% of the MS runs. Since a fully sulfated heparin octasaccharide can contain up to 12 sulfates, this indicated that the active octasaccharide is considerably undersulfated. No material exhibiting more than eight sulfates or monosaccharides could be detected in independent analyses from at least three preparations. The absence of detectable mass greater than the indicated peaks in the complete spectrum that detects picogram levels of mass ranging from 2,000 to 9,000 Da confirmed the purity of the octasaccharide in respect to length. Notably no mass peaks indicative of the presence of acetyl groups in the moderate and high affinity octasaccharide fractions were evident. Acetyl groups were present in the unretained and low affinity fractions from FGF7 chromatography (not shown).

The MALDI-TOF analysis confirmed that the more abundant inactive octasaccharides with moderate affinity for FGF7 were expectedly more heterogeneous (Fig. 10, lower panel). Components bearing 8–12 sulfates were present with predominant 11- and 12-sulfated octasaccharide peaks at m/z 2,229.0 and 2,309.28, respectively. This indicates that similar to the high affinity antithrombin-binding motif [Hurst et al., 1979; Petitou et al., 2003], the active oligosaccharide motif with highest affinity for FGF7 is not a simple correlate of increasing sulfation and charge density. On the contrary, high specific activity is related to the specific distribution of less than a maximum number of sulfates and possibly other elements unrelated to anionic charge required for optimum interaction with the heparin-binding domains of both FGF7 and FGFR2IIIb. Moreover, the common and highly sulfated octasac-

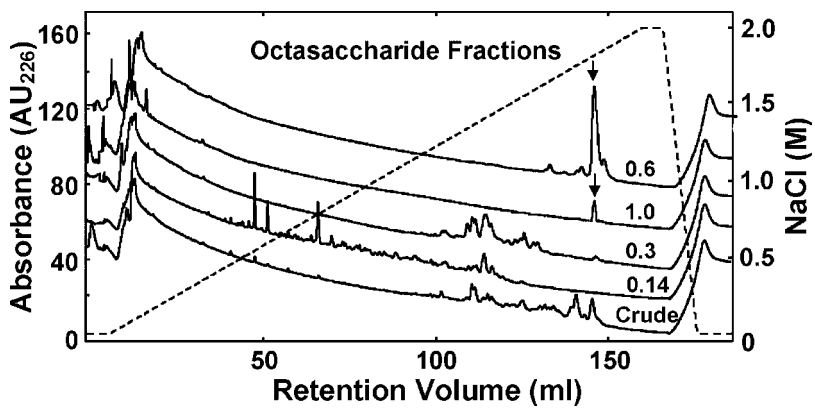

Fig. 9. Strong anion exchange chromatography (SAX) of octasaccharide fractions from FGF7 affinity columns. Crude octasaccharide and fractions for FGF7 were applied to SAX at 100 μg except only 10 μg of the high affinity octasaccharide was committed to the analysis to conserve limited material. The column was eluted with the indicated gradient of NaCl (dotted line) (Materials and Methods). Arrows indicate major peaks from the moderate and high affinity octasaccharides that were utilized for activity and structural analysis. The trace for the high affinity octasaccharide was placed below the moderate affinity fraction for clarity. The specific data presented is representative of three chromatograms performed for each of three independent preparations using independent GST-FGF7 affinity columns.

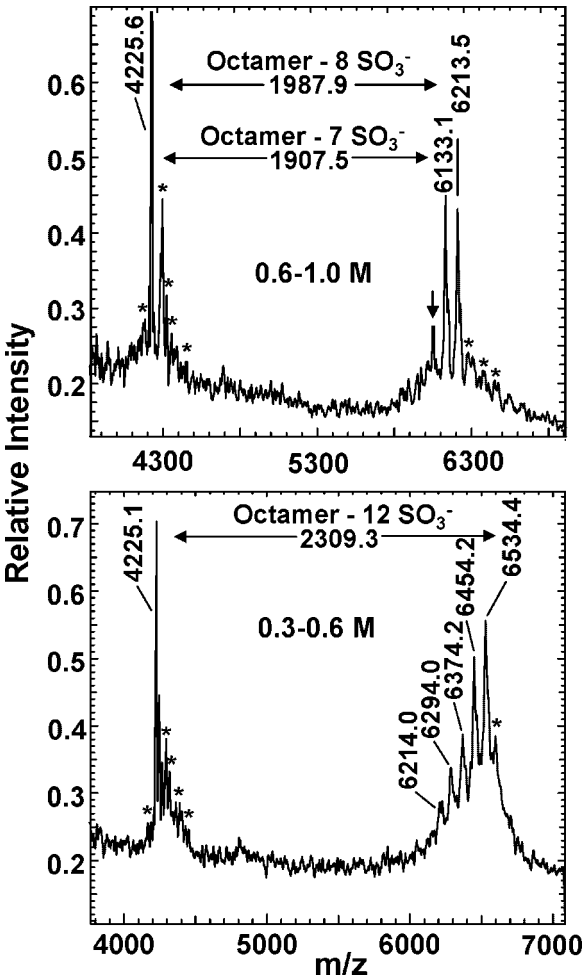

Fig. 10. MALDI-TOF-MS analysis of high and moderate affinity octasaccharides for FGF7. **A**: High affinity octasaccharides for FGF7. Arrow, peak coincident in mass with an octasaccharide bearing 6 sulfates. **B**: Abundant moderate affinity octasaccharides for FGF7. Mass peaks from left to right indicate octasaccharides bearing 8, 9, 10, 11, and 12 sulfates. Peaks are labeled with m/z values and calculation of mass in Dalton of octasaccharides bearing 7, 8 (A) and 12 (B) sulfates is indicated. Asterisks indicate impurities in the peptide carrier or their complex with the oligosaccharides. The data are representative of analyses using three independent preparations of oligosaccharide and GST-FGF7.

charides with less affinity for FGF7 are inactive in assembly of the FGFR2IIIb complex.

Disaccharide composition of the 7,8-S-octasaccharide mixture we refer to as 7,8-S-OctaF7 was determined by SAX-HPLC, IPRP-HPLC, and MALDI-TOF-MS. The SAX analysis revealed the presence at 0.3M NaCl of the relatively rare N-unsubstituted bisulfated disaccharide, ΔHexA2SGlcN6S, and a trisulfated disaccharide coincident with the ΔHexA2SGlcNS6S standard at 0.95M NaCl (Fig. 11A). The two components were present at an estimated ratio of 2:1. Analysis of the digest by IPRP-HPLC gave rise to the same two disaccharides in about a 2:1 ratio (Fig. 11B). A trisulfated disaccharide in 7,8-S-OctaF7 is a candidate for GlcAGlcNS3S6S required for the observed levels of anticoagulant activity [Capila and Linhardt, 2002; Petitou et al., 2003]. Unavailability of homogenous disaccharide standards containing 3-*O*-sulfate precluded a conclusion on whether 3-*O*-sulfate containing bi- or trisulfated disaccharides can be separated from those with sulfates on alternate positions. Separate experiments indicated that the major disaccharides ΔHexAGlcNS3S6S and ΔHexA2SGlcNS6S from a digest of the synthetic anticoagulant pentasaccharide AT5 overlapped with each other and the ΔHexA2SGlcNS6S standard on SAX (results not shown). In contrast to 7,8-S-OctaF7, the more abundant heterogeneous and inactive octasaccharides with moderate affinity for FGF7 were comprised of predominately a trisulfated disaccharide (Fig. 11C) with trace peaks of less sulfated disaccharides distributed along the gradient.

Combinations of ΔHexA2SGlcN6S and trisulfated disaccharide in a 2:1 ratio can only yield 9-, 10- or 11-sulfated octasaccharides. This is inconsistent with the 7- or 8-sulfated octasaccharides that make up the 7,8-S-OctaF7 mixture and the observed level of anticoagulant activity. The presence of a third unsulfated or monosulfated disaccharide could account for the 7- and 8-sulfated saccharides. However, no single peak coincident with an unsulfated disaccharide or three types of monosulfated disaccharide standards were evident across the early parts of the SAX- and IPRP-HPLC gradient analyses (Fig. 11). Therefore, although MALDI-TOF-MS cannot detect an unsulfated species, it was employed to test for the presence of a monosulfated disaccharide. The analysis revealed the expected signals with m/z values of 577.46 and 496.71 for disaccharides with three and two sulfates (Fig. 12). A third peak (arrow) confirmed the presence of a monosulfated disaccharide. Taken together these results indicate that 7,8-S-OctaF7 may be comprised of two ΔHexA2SGlcN6S units, one trisulfated disaccharide, and a third type of disaccharide that is variably sulfated to yield an unsulfated and monosulfated mixture. The monosulfated component may be distributed among diverse positions that preclude detection of any one single disaccharide in the chromatographic analyses. The 7-S-octasaccharide would contain the unsulfated disacchar-

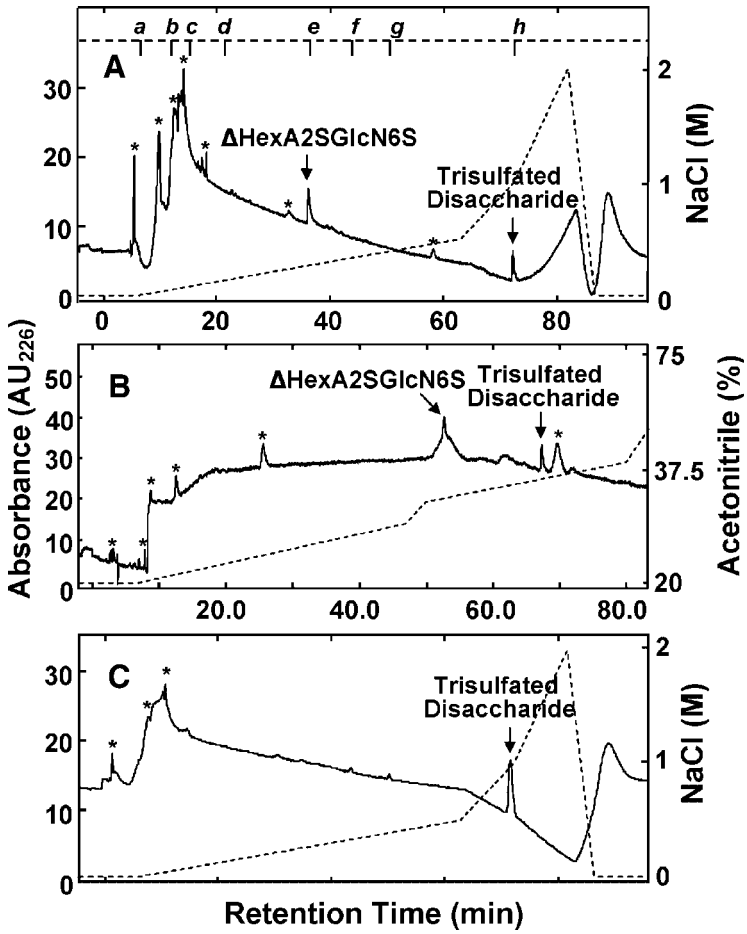

Fig. 11. Disaccharide composition of the 7,8-S-OctaF7 and moderate affinity octasaccharides. **A**: SAX analysis of disaccharides from 7,8-S-OctaF7. The analysis was the same as described in Figure 9 except a different NaCl elution gradient was employed (dotted line). **B**: IPRP-HPLC analysis of disaccharides from 7,8-S-OctaF7 (Materials and Methods). **C:** SAX analysis of a digest of the moderate affinity octasaccharides. About 2 μg of the 7,8-S-OctaF7 and 5 μg of the 0.60M eluate were reduced to disaccharides prior to application of the mixture to the indicated columns. The elution position of disaccharide standards is shown in A. Asterisks indicate solvent peaks. a, ΔHexAGlcN; b, ΔHexA2SGlcN; c, ΔHexAGlcN6S; d, ΔHexAGlcNS; e, ΔHexA2SGlcN6S; f, ΔHexAGlcNS6S; g, ΔHexA2SGlcNS; h, ΔHexA2SGlcNS6S. Five N-acetylated standards employed are not shown. Data shown are representative of three reproductions from digestion of each of three independent oligosaccharide preparations.

ide and the 8-S-octasaccharide the monosulfated disaccharide. It is noteworthy that the 7-S-octasaccharide appears more abundant in the mixture than the 8-S-octasaccharide despite the fact that peak yield usually varies inversely with degree of sulfation in the MALDI-TOF analysis (Fig. 10). This may indicate that the 7-S-octasaccharide is the minimum requirement for high affinity for FGF7 and complex formation with FGFR2IIIb. A 6-*O*-sulfate on the monsulfated disaccharide in the 8-S-octasaccharide most likely underlies the observed anticoagulant activity [Linhardt, 2003]. It may be inconsequential to the FGF7, octasaccharide–FGR2IIIb or FGF7–octasaccharide–FGFR2IIIb interactions.

DISCUSSION

Here we show that a crude heparin octasaccharide can be purified to 7- and 8-sulfated components (7,8-S-OctaF7) by FGF7 bioaffinity based on resistance to salt above 0.60M. The rare 7,8-S-OctaF7 (0.7% of crude octasaccharides) exhibits highest specific activity in support of a dimeric complex of FGF7-7,8-S-OctaF7-FGFR2IIIb. It is also enriched in anticoagulant activity based on antithrombin-mediated inhibition of Factor Xa. The mixture is structurally distinct and characterized by the rare N-unsubstituted bisulfated disaccharide ΔHexA2SGlcN6S, a trisulfated disaccharide, and

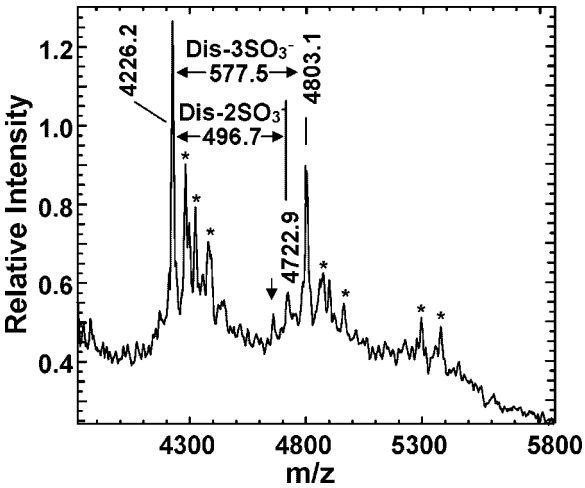

Fig. 12. Analysis of disaccharides from 7,8-S-OctaF7 by MALDI-TOF-MS. A sample of 2 μg of 7,8-S-OctaF7 mixture was reduced to disaccharides (Materials and Methods) and about 10% of the digest mixture was subjected to replicate MALDI-TOF-MS analysis. Trisulfated (DIS-3SO3) and disulfated (DIS-2SO3) disaccharide peaks are indicated. Asterisks indicate peaks due to minor heterogeneity caused by the carrier peptide. Arrow, peak with mass of a monosulfated disaccharide. Data shown are representative of about 10 spectra run from each of three independent preparations of 7,8-S-Octa7 with independent GST-FGF affinity columns and oligosaccharide preparations.

probably a variably monosulfated or unsulfated disaccharide. The trisulfated disaccharide is most likely GlcAGlcNS3S6S presumably required for the observed level of anticoagulant activity. In contrast to the relatively homogeneous and rare 7,8-S-OctaF7 mixture, more abundant octasaccharides (39% of the crude octasaccharide) with moderate affinity for FGF7 were much more heterogeneous and highly sulfated. Octasaccharides with moderate affinity exhibited predominantly 11- and 12-sulfated components comprised of predominately a trisulfated disaccharide. This was most likely ΔHexA2SGlcNS6S, the most common disaccharide in heparin and HS. This suggests that HS motifs with high affinity for FGF7 and other FGFs with similarly unique heparin-binding domains may not be simply proportional to high total charge density and degree of sulfation. Instead they require a less than fully sulfated motif in which both sulfated and unsulfated groups are specifically distributed.

The surprising fact that complexes of FGF7 with more highly sulfated octasaccharides exhibit lower salt resistance than undersulfated 7,8-S-OctaF7 is consistent with a requirement for precise interaction of the saccharide sequence with the reduced and dispersed basic groups within the heparin-binding domain of FGF7. The opposing charge or steric conflict of fully sulfated chains with intervening acidic or uncharged residues may contribute to the reduction in affinity. This high degree of specificity exhibited by FGF7 is in contrast to results of a similar analysis of the interaction of the crude heparin [Luo et al., 2003] and heparin oligosaccharides with FGF1 (manuscript in preparation). A much wider range of heparin oligosaccharides binds with high affinity to FGF1 based on salt resistance. The graded increase in affinity appears largely proportional to an increase in total charge density. Analysis of the topography and condensed basicity of the heparin-binding domains of FGF2, FGF4, FGF8, and FGF10 also predict that they may bind a much wider range of highly charged oligosaccharide motifs with high affinity. Our results support conclusions significantly different from the generalization that all FGF, FGFR, and FGF-FGFR composites share a broad range of HS motifs [Kreuger et al., 2005]. They conflict with suggestions that variation in the FGF–HS interaction is simply proportional to variations in charge density without discrimination of disposition of saccharides and sulfate groups. The conflicting results may lie in differences in oligosaccharide source material, particularly fully N-sulfated oligosaccharide libraries, and specific bioactivity of FGFs and FGFR in respect to affinity for HS motifs.

Because of its abundance and availability, heparin, a highly sulfated form of HS, is a widely applied biochemical indicator of the role of HS from diverse tissue sources in control of FGF family signaling and functions of other proteins [Powell et al., 2004; Yates et al., 2004]. PIMH was used in this study because of its availability for biochemical studies and high glucuronic acid content that most closely mimics the spectrum of tissue HS [Yates et al., 2004]. We interpret our results to reflect different roles of tissue matrix and cell surface HS motifs in control of FGF family signaling. Rare, undersulfated, and structurally specific motifs with high affinity for FGF7 are those directly involved in formation of a complex of FGF7 and FGFR2IIIb and transmembrane signaling. They are unlikely widely shared by other FGFs. The more abundant and highly sulfated fractions with moderate affinity represent FGFR-independent sites that control stability, intercellular trafficking, and access of

FGF7 to membrane FGFR2IIIb. Although these interactions are likely dominated by overall charge density and the surface charge of FGF, motifs with moderate affinity may show some selectivity among FGFs due to differences in net basicity and structure of heparin-binding domains, but are likely to be shared among FGFs. The low affinity and less highly sulfated class may simply represent non-specific polyelectrolyte–protein interactions. In a physiological context this may contribute to FGF gradients in a tissue setting dependent on the overall surface charge of the FGF. The net activity of a particular FGF in a specific tissue environment is likely determined by the relative abundance and location of these three classes of HS sites and their competition for FGF and FGFR.

The order of assembly, stoichiometry among subunits, and mode of activation of the oligomeric FGF signaling complex is unclear. Crystal structures and kinetic analysis in solution using soluble recombinant FGF, FGFR ectodomains, and generic fully sulfated heparin oligosaccharides have produced irreconcilable structural models of the oligomeric FGF–HS–FGFR complex [Pellegrini et al., 2000; Schlessinger et al., 2000]. Analysis of assembly of the FGF–HS–FGFR complex in solution is hampered by the lack of dependence of the binding of FGF to FGFR on HS and the low affinity of soluble FGFR for HS. Therefore, results of solution analyses are biased toward models of assembly of FGF–HS–FGFR complexes from HS-independent complexes of FGF–FGFR. The use of soluble FGFR ectodomains with low affinity for HS further biases against assembly from obligatory preexistent complexes of HS–FGFR into which FGF docks. One model from solution studies suggests that a complex of FGF-HS docks onto a free FGFR or an HS chain docks onto an FGF–FGFR complex to form a ternary FGF–HS–FGFR complex [Ibrahimi et al., 2004]. Two FGF–HS–FGFR complexes then dimerize to form an oligomeric unit with 2:2:2 stoichiometry [Pellegrini et al., 2000; Schlessinger et al., 2000]. Recently a refinement of this model has been suggested where two HS chains dock into a symmetric dimer of two FGF–FGFR complexes [Mohammadi et al., 2005]. An opposing model is also supported by X-ray crystallography and solution kinetic analysis, but is still based on assembly from HS-independent FGF–FGFR complexes [Harmer et al., 2004a; Pellegrini et al., 2000]. One HS chain interacts with an FGF-FGFR unit to form an FGF–HS–FGFR complex. The latter then interacts asymmetrically with another FGF-FGFR unit to form an oligomeric complex of 2:1:2 FGF:HS:FGFR stoichiometry.

In the tissue environment, HS is in large excess to FGFR at a molar ratio of HS proteoglycans to FGFR of 20 to 200 on the cell surface alone [Powell et al., 2002]. In a physiological context it is probable that whether free or as a complex of HS-FGF, FGF encounters a complex of HS–FGFR. In contrast to soluble FGFR ectodomains, membrane- or bead-anchored recombinant eukaryotic FGFR dimers comprised of the ectodomain, the extracellular juxtamembrane, and transmembrane domains are dependent on HS for binding of FGF. The anchored dimeric FGFR also bind HS with high affinity (Kd $<$10 nM) independent of FGF [Kan et al., 1996]. They also select a minor subset of total HS that is enriched in anticoagulant activity [McKeehan et al., 1999]. The interaction forms FGFR–HS complexes that are highly selective for binding of different FGFs dependent on FGFR isotype and cell context [Kan et al., 1999]. This indicates that under physiological conditions where FGFR and HS chains are anchored in cell membranes, dimeric complexes of FGFR-HS [Kan et al., 1996] may exist that exhibit high affinity for FGF to form the active oligomeric FGF–HS–FGFR signaling complex.

In this study, we show that similar to motifs that interact with FGFR, the high affinity HS motif(s) for FGF7 are also rare and enriched in anticoagulant activity. The highly purified 7,8-S-OctaF7 octasaccharide reported here forms a complex with FGFR2IIIb dimers that then supports binding of FGF7 to form FGF7-7,8-S-OctaF7–FGFR2IIIb complexes. A complex of the ectodomain of FGFR2IIIb and 7,8-S-OctaF7, both of which are independently specific for and have high affinity for FGF7, is potentially the most selective and most competitive composite site for FGF7 among the total FGF7 binding sites in the extracellular environment. Our observations favor a model where FGF7 exchanges from sites comprised of the abundant matrix HS motifs with lower affinity than 7,8-S-Octa7 into dimeric complexes of FGFR2IIIb–7,8-S-OctaF7.

In nature, FGF7 generally acts in paracrine mode and originates in cells separated from

those expressing FGFR2IIIb by the tissue matrix and a basement membrane. Whether FGF7 exchanges from lower affinity HS onto FGFR2IIIb–7,8-S-OctaF7 complexes or a complex of FGF7–7,8-S-OctaF7 exchanges with complexes of FGFR2IIIb and HS with less specificity and affinity for FGF7 depends on location of the high affinity 7,8-S-OctaF7 sites. If extracellular matrix sites are immobile and FGF7 moves among extracellular matrix sites by competition and exchange from one site to another, the probability that FGF7 can reach cell surface FGFR2IIIb once it encounters high affinity 7,8-S-OctaF7 in the matrix is low. If solubilized by enzymatic action in the extracellular environment, complexes of 7,8-S-OctaF7–FGF7 would be highly competitive for cell surface complexes of FGFR2IIIb and HS with lower affinity than 7,8-S-OctaF7-FGF7 for FGF7. However, unless solubilization of extracellular matrix 7,8-S-OctaF7–FGF7 complexes is selective, the unlikely event of large-scale solubilization of HS sites in the matrix would be required since 7,8-S-OctaF7 motifs are rare. We predict that the rare 7,8-S-OctF7 motifs in the total matrix environment reside in cell membrane complexes with FGFR2IIIb rather than dispersed in the tissue matrix.

In conclusion, as predicted from the unique structural features of the heparin-binding domain of FGF7 [Ye et al., 2001], a less than fully sulfated octasaccharide motif with seven and eight specifically distributed sulfates is required for the high affinity interaction with FGF7. Combined SAX-HPLC, IPRP-HPLC, and MALDI-TOF-MS disaccharide and anticoagulant activity analyses suggested a composition of two ΔHexA2SGlcN6S, one trisulfated trisaccharide, and one variably unsulfated/monosulfated disaccharide. The trisulfated disaccharide is the candidate for GlcAGlcNS3S6S, the 3-*O* sulfate of which is critical for anticoagulant activity [Capila and Linhardt, 2002]. The most abundant 7-S-octasaccharide in the mixture may contain the unsulfated disaccharide and be the minimal requirements for high affinity binding to FGF7 and the formation of the FGF7–HS–FGFR2IIIb complex. All conceivable arrangements of the putative two ΔHexA2SGlcN6S, GlcAGlcNS3S6S and an unsulfated disaccharide within the 7-S-octasaccharide are insufficient to explain the elevated level of anticoagulant activity. A 6-*O*-monosulfated disaccharide adjacent to GlcAGlcNS3S6S on the non-reducing side is required [Linhardt, 2003; Petitou et al., 2003]. If part of the monosulfated disaccharide in the 8-S-octasaccharide is a 6-*O*-sulfate, then conceivable arrangements of the minimal 4-sulfate and two carboxyl groups for a pentasaccharide sequence within the 8-S-octasaccharide would meet requirements [Linhardt, 2003; Petitou et al., 2003]. If the monosulfation is dispensable for high affinity FGF7 binding and complex assembly, then all elements in the anticoagulant pentasaccharide per se are unlikely required. The fact that the synthetic anticoagulant pentasaccharide AT5 fails to support formation of the FGF7–HS–FGFR2IIIb complex further indicates that different structural features in respect to length or distribution of groups in 7,8-S-OctaF7 are required.

Arrangements of two N-unsubstituted GlcN and a monosulfated or unsulfated disaccharide flanking a trisulfated disaccharide within undersulfated octasaccharide motifs are consistent with specific disposition of sulfate groups for optimal fit with the dispersed basic clusters of the FGF7 heparin-binding interface [Ye et al., 2001]. Properly positioned unsulfated groups may be equally important to avoid conflict with intervening uncharged or acidic groups on the FGF7 interface that reduce affinity. Disposition of sulfate residues may be less stringent for interaction with FGF when the heparin-binding domain is comprised of a single condensed area of positive charge as observed in FGF1, FGF2, FGF4, FGF8, and FGF10. Arrangements of the three types of disaccharides within undersulfated octasaccharide motifs also meet requirements for high affinity interaction with FGFR2IIIb and interactions in the FGF7–HS–FGFR2IIIb complex.

Complete sequence analysis is essential for elucidation of the precise arrangement of groups within the octasaccharide and to guide group-specific modifications and synthesis for further determination of the minimum structure and contribution of each group to activity. Results to be reported in detail elsewhere reveal that the 7,8-S-OctaF7 mixture specifically supports FGF7-induced proliferation of HS-depleted keratinocytes expressing FGFR2IIIb. It fails to support FGF1-induced proliferation of stromal fibroblasts expressing FGFR1. In contrast, highly charged and heterogeneous octasaccharide mixtures with either high affinity for FGF1 or moderate

affinity for FGF7 support the response of both cell types to FGF1, but not FGF7. We predict that FGF and FGFR isotype-specific oligosaccharide motifs will contribute to clarification of the nature and order of assembly of FGF signaling complexes derived from diverse members of the FGF and FGFR family. They will also be useful as a structural base for building high affinity agonists and antagonists of FGF signaling for pharmaceutical intervention.

ACKNOWLEDGMENTS

We thank Dr. Robert Linhardt for providing the synthetic antithrombin-binding pentasaccharide and helpful advice.

REFERENCES

Berman B, Ostrovsky O, Shlissel M, Lang T, Regan D, Vlodavsky I, Ishai-Michaeli R, Ron D. 1999. Similarities and differences between the effects of heparin and glypican-1 on the bioactivity of acidic fibroblast growth factor and the keratinocyte growth factor. J Biol Chem 274:36132–36138.

Capila I, Linhardt RJ. 2002. Heparin-protein interactions. Angew Chem Int Ed Engl 41:391–412.

Esko JD, Selleck SB. 2002. Order out of chaos: Assembly of ligand binding sites in heparan sulfate. Annu Rev Biochem 71:435–471.

Guimond SE, Turnbull JE. 1999. Fibroblast growth factor receptor signalling is dictated by specific heparan sulphate saccharides. Curr Biol 9:1343–1346.

Harmer NJ, Ilag LL, Mulloy B, Pellegrini L, Robinson CV, Blundell TL. 2004a. Towards a resolution of the stoichiometry of the fibroblast growth factor (FGF)-FGF receptor-heparin complex. J Mol Biol 339:821–834.

Harmer NJ, Pellegrini L, Chirgadze D, Fernandez-Recio J, Blundell TL. 2004b. The crystal structure of fibroblast growth factor (FGF) 19 reveals novel features of the FGF family and offers a structural basis for its unusual receptor affinity. Biochemistry 43:629–640.

Hurst RE, Menter JM, West SS, Settine JM, Coyne EH. 1979. Structural basis for the anticoagulant activity of heparin. 1. Relationship to the number of charged groups. Biochemistry 18:4283–4287.

Ibrahimi OA, Zhang F, Hrstka SC, Mohammadi M, Linhardt RJ. 2004. Kinetic model for FGF, FGFR, and proteoglycan signal transduction complex assembly. Biochemistry 43:4724–4730.

Itoh N, Ornitz DM. 2004. Evolution of the Fgf and Fgfr gene families. Trends Genet 20:563–569.

Juhasz P, Biemann K. 1995. Utility of non-covalent complexes in the matrix-assisted laser desorption ionization mass spectrometry of heparin-derived oligosaccharides. Carbohydr Res 270:131–147.

Kan M, Shi EG, McKeehan WL. 1991. Identification and assay of fibroblast growth factor receptors. Methods Enzymol 198:158–171.

Kan M, Wang F, Xu J, Crabb JW, Hou J, McKeehan WL. 1993. An essential heparin-binding domain in the fibroblast growth factor receptor kinase. Science 259:1918–1921.

Kan M, Wang F, To B, Gabriel JL, McKeehan WL. 1996. Divalent cations and heparin/heparan sulfate cooperate to control assembly and activity of the fibroblast growth factor receptor complex. J Biol Chem 271:26143–26148.

Kan M, Wu X, Wang F, McKeehan WL. 1999. Specificity for fibroblast growth factors determined by heparan sulfate in a binary complex with the receptor kinase. J Biol Chem 274:15947–15952.

Kan M, Uematsu F, Wu X, Wang F. 2001. Directional specificity of prostate stromal to epithelial cell communication via FGF7/FGFR2 is set by cell- and FGFR2 isoform-specific heparan sulfate. In Vitro Cell Devel Biol-Animal 37:575–577.

Kreuger J, Salmivirta M, Sturiale L, Gimenez-Gallego G, Lindahl U. 2001. Sequence analysis of heparan sulfate epitopes with graded affinities for fibroblast growth factors 1 and 2. J Biol Chem 276:30744–30752.

Kreuger J, Jemth P, Sanders-Lindberg E, Eliahu L, Ron D, Basilico C, Salmivirta M, Lindahl U. 2005. Fibroblast growth factors share binding sites in heparan sulphate. Biochem J 389:145–150.

Kuberan B, Lech MZ, Beeler DL, Wu ZL, Rosenberg RD. 2003. Enzymatic synthesis of antithrombin III-binding heparan sulfate pentasaccharide. Nat Biotechnol 21:1343–1346.

LaRochelle WJ, Sakaguchi K, Atabey N, Cheon HG, Takagi Y, Kinaia T, Day RM, Miki T, Burgess WH, Bottaro DP. 1999. Heparan sulfate proteoglycan modulates keratinocyte growth factor signaling through interaction with both ligand and receptor. Biochemistry 38:1765–1771.

Lindahl U, Kusche-Gullberg M, Kjellen L. 1998. Regulated diversity of heparan sulfate. J Biol Chem 273: 24979–24982.

Linhardt RJ. 2003. 2003 Claude S. Hudson Award address in carbohydrate chemistry. Heparin: Structure and activity. J Med Chem 46:2551–2564.

Loo BB, Darwish KK, Vainikka SS, Saarikettu JJ, Vihko PP, Hermonen JJ, Goldman AA, Alitalo KK, Jalkanen MM. 2000. Production and characterization of the extracellular domain of recombinant human fibroblast growth factor receptor 4. Int J Biochem Cell Biol 32:489–497.

Loo BM, Kreuger J, Jalkanen M, Lindahl U, Salmivirta M. 2001. Binding of heparin/heparan sulfate to fibroblast growth factor receptor 4. J Biol Chem 276:16868–16876.

Luo Y, Cho HH, McKeehan WL. 2003. Biospecific extraction and Neutralization of anticoagulant heparin with fibroblast growth factors (FGF). J Pharm Sci 92:2117–2127.

Luo Y, Cho HH, Jones RB, Jin C, McKeehan WL. 2004. Improved production of recombinant fibroblast growth factor 7 (FGF7/KGF) from bacteria in high magnesium chloride. Protein Expr Purif 33:326–331.

McKeehan WL, Wang F, Kan M. 1998. The heparan sulfate-fibroblast growth factor family: Diversity of structure and function. Prog Nucleic Acid Res Mol Biol 59:135–176.

McKeehan WL, Wu X, Kan M. 1999. Requirement for anticoagulant heparan sulfate in the fibroblast growth factor receptor complex. J Biol Chem 274:21511–21514.

Mohammadi M, Olsen SK, Goetz R. 2005. A protein canyon in the FGF-FGF receptor dimer selects from an a la carte

menu of heparan sulfate motifs. Curr Opin Struct Biol 15:506–516.

Ornitz DM. 2000. FGFs, heparan sulfate and FGFRs: Complex interactions essential for development. Bioessays 22:108–112.

Ostrovsky O, Berman B, Gallagher J, Mulloy B, Fernig DG, Delehedde M, Ron D. 2002. Differential effects of heparin saccharides on the formation of specific fibroblast growth factor (FGF) and FGF receptor complexes. J Biol Chem 277:2444–2453.

Pellegrini L, Burke DF, von Delft F, Mulloy B, Blundell TL. 2000. Crystal structure of fibroblast growth factor receptor ectodomain bound to ligand and heparin. Nature 407:1029–1034.

Petitou M, Casu B, Lindahl U. 2003. 1976–1983, a critical period in the history of heparin: The discoveryof the antithrombin binding site. Biochimie 85:83–89.

Plotnikov AN, Eliseenkova AV, Ibrahimi OA, Shriver Z, Sasisekharan R, Lemmon MA, Mohammadi M. 2001. Crystal structure of fibroblast growth factor 9 reveals regions implicated in dimerization and autoinhibition. J Biol Chem 276:4322–4329.

Powell AK, Fernig DG, Turnbull JE. 2002. Fibroblast growth factor receptors 1 and 2 interact differently with heparin/heparan sulfate. Implications for dynamic assembly of a ternary signaling complex. J Biol Chem 277:28554–28563.

Powell AK, Yates EA, Fernig DG, Turnbull JE. 2004. Interactions of heparin/heparan sulfate with proteins: Appraisal of structural factors and experimental approaches. Glycobiology 14:17R–30R.

Schlessinger J, Plotnikov AN, Ibrahimi OA, Eliseenkova AV, Yeh BK, Yayon A, Linhardt RJ, Mohammadi M. 2000. Crystal structure of a ternary FGF-FGFR-heparin complex reveals a dual role for heparin in FGFR binding and dimerization. Mol Cell 6:743–750.

Shriver Z, Sundaram M, Venkataraman G, Fareed J, Linhardt R, Biemann K, Sasisekharan R. 2000. Cleavage of the antithrombin III binding site in heparin by heparinases and its implication in the generation of low molecular weight heparin. Proc Natl Acad Sci USA 97:10365–10370.

Wang F, Kan M, Xu J, Yan G, McKeehan WL. 1995. Ligand-specific structural domains in the fibroblast growth factor receptor. J Biol Chem 270:10222–10230.

Wu ZL, Zhang L, Yabe T, Kuberan B, Beeler DL, Love A, Rosenberg RD. 2003. The involvement of heparan sulfate (HS) in FGF1/HS/FGFR1 signaling complex. J Biol Chem 278:17121–17129.

Yates EA, Guimond SE, Turnbull JE. 2004. Highly diverse heparan sulfate analogue libraries: Providing access to expanded areas of sequence space for bioactivity screening. J Med Chem 47:277–280.

Ye S, Luo Y, Lu W, Jones RB, Linhardt RJ, Capila I, Toida T, Kan M, Pelletier H, McKeehan WL. 2001. Structural basis for interaction of FGF-1, FGF-2, and FGF-7 with different heparan sulfate motifs. Biochemistry 40: 14429–14439.